

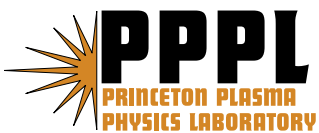
PPPL-4160

PPPL-4160

**Observation of Instability-induced Current  
Redistribution in a Spherical Torus Plasma**

J.E. Menard, R.E. Bell, S.M. Kaye,  
B.P. LeBlanc, F.M. Levinton, S.S. Medley,  
D. Stutman, K. Tritz, and H. Yuh

May 2006



# **Princeton Plasma Physics Laboratory**

## **Report Disclaimers**

---

### **Full Legal Disclaimer**

This report was prepared as an account of work sponsored by an agency of the United States Government. Neither the United States Government nor any agency thereof, nor any of their employees, nor any of their contractors, subcontractors or their employees, makes any warranty, express or implied, or assumes any legal liability or responsibility for the accuracy, completeness, or any third party's use or the results of such use of any information, apparatus, product, or process disclosed, or represents that its use would not infringe privately owned rights. Reference herein to any specific commercial product, process, or service by trade name, trademark, manufacturer, or otherwise, does not necessarily constitute or imply its endorsement, recommendation, or favoring by the United States Government or any agency thereof or its contractors or subcontractors. The views and opinions of authors expressed herein do not necessarily state or reflect those of the United States Government or any agency thereof.

### **Trademark Disclaimer**

Reference herein to any specific commercial product, process, or service by trade name, trademark, manufacturer, or otherwise, does not necessarily constitute or imply its endorsement, recommendation, or favoring by the United States Government or any agency thereof or its contractors or subcontractors.

## **PPPL Report Availability**

---

### **Princeton Plasma Physics Laboratory**

This report is posted on the U.S. Department of Energy's Princeton Plasma Physics Laboratory Publications and Reports web site in Fiscal Year 2006.

The home page for PPPL Reports and Publications is:

[http://www.pppl.gov/pub\\_report/](http://www.pppl.gov/pub_report/)

### **Office of Scientific and Technical Information (OSTI):**

Available electronically at: <http://www.osti.gov/bridge>.

Available for a processing fee to U.S. Department of Energy and its contractors, in paper from:

U.S. Department of Energy  
Office of Scientific and Technical Information  
P.O. Box 62  
Oak Ridge, TN 37831-0062

Telephone: (865) 576-8401

Fax: (865) 576-5728

E-mail: [reports@adonis.osti.gov](mailto:reports@adonis.osti.gov)

# Observation of Instability-induced Current Redistribution in a Spherical Torus Plasma

J.E. Menard<sup>1</sup>, R.E. Bell<sup>1</sup>, S.M. Kaye<sup>1</sup>, B.P. LeBlanc<sup>1</sup>, F.M. Levinton<sup>2</sup>, S.S. Medley<sup>1</sup>, D. Stutman<sup>3</sup>, K. Tritz<sup>3</sup>, H. Yuh<sup>2</sup>

<sup>1</sup>*Princeton Plasma Physics Laboratory,*

*Princeton, New Jersey*

<sup>2</sup>*Nova Photonics Inc.,*

*Princeton, New Jersey*

<sup>3</sup>*Johns Hopkins University,*

*Baltimore, Maryland*

(Dated: April 16, 2006)

## Abstract

A novel Motional Stark Effect diagnostic has been utilized to reconstruct the parallel current density profile in a spherical torus plasma for the first time. The measured current profile compares favorably with neoclassical theory when no large-scale MHD instabilities are present in the plasma. However, in discharges with sustained high fraction of non-inductive current drive, a current profile anomaly is observed during saturated interchange instability activity. Neutral beam injection current drive redistribution can account for the apparent anomaly and contributes to sustaining the central safety factor above unity for over five current redistribution times.

PACS numbers: 52.55.Fa, 52.55.Wq

The Spherical Torus (ST) configuration [1] has made considerable progress in achieving good confinement in the H-mode confinement regime [2] and high toroidal beta [3–6] required for efficient fusion energy applications. Recent progress has also been achieved in integrating high confinement, high plasma shaping factor, and stable operation above the no-wall stability limit to achieve high non-inductive current fraction [7–9]. High non-inductive current fraction is deemed essential for the ST concept due to the necessarily compact central column and transformer used for inductive current drive. Advanced tokamaks have recently achieved high toroidal beta with high non-inductive current fraction [10] utilizing a combination of bootstrap current [11], neutral beam injection current drive (NBICD), and electron cyclotron current drive. However, given the difficulty in achieving fully non-inductive operation at high beta, alternative discharge scenarios have also been developed in which a majority of the current is driven by the neoclassical bootstrap effect, but ohmic current drive is still a significant fraction of the total current [12–14]. A necessary element of these scenarios is avoidance of large sawtooth instabilities which might otherwise trigger potentially disruptive 2/1 neoclassical tearing modes (NTMs). In tokamak devices that minimize the impact of the sawtooth, the central safety factor  $q_0$  is maintained at or just above unity either through auxiliary current drive or via MHD instabilities which apparently redistribute current. A key scientific element of understanding current drive physics in the absence of MHD activity has been the validation of neoclassical resistivity, bootstrap current, and other sources of non-inductive current coupled with measurements of the internal inductive electric field [15].

In this article we report on the first systematic validation of neoclassical and beam-driven currents in low aspect tokamak plasmas. These studies are made possible by a novel Motional Stark Effect (MSE) diagnostic technique [16] developed specifically for the low magnetic field strength ( $B_T \leq 0.6T$ ) of present-day ST devices. Similar to standard aspect ratio tokamaks, NSTX has also now demonstrated discharge scenarios in which a majority of the current is driven non-inductively and the central  $q$  is maintained at or above unity for durations limited only by coil heating limits. In NSTX, this condition is made possible initially by operation at high normalized beta  $\equiv \beta_N$  and bootstrap fraction, and is later facilitated by the presence of saturated MHD activity in the plasma core. As described below, the broad current profile measured during this MHD activity apparently results from redistribution of injected energetic particles.

The first step in any analysis of current profile evolution is accurate reconstruction of the time-evolving equilibria. The NSTX MSE system for the data analyzed here consists of 8 midplane channels covering the inner 90% of the plasma normalized minor radius  $\rho \equiv \hat{\psi}_{pol}^{1/2}$ . The reconstructed current profiles are most accurate in the plasma core since 7 of the 8 channels are typically inside  $\rho = 0.6$ . A 51 point midplane horizontally viewing C-VI impurity charge exchange recombination spectroscopy system is used to determine the electric field profile from impurity radial force balance to correct the MSE pitch angle data [17]. In addition, the electron temperature is assumed to be a magnetic flux function and is used as an additional constraint which modifies the plasma boundary location by up to several centimeters. This improved boundary identification improves the mapping of all kinetic profiles to flux functions and improves the accuracy of the calculated current drive sources [18]. Plasma toroidal rotation has previously been shown to cause the density profile to deviate from a flux function in NSTX plasmas [19], and flux-surface-averaged kinetic profiles are used in the evaluation of neoclassical terms [20]. Toroidal rotation slightly decreases the reconstructed  $q_{min}$  ( $\Delta q_{min} = -0.1-0.15$  for peak sonic Mach number  $M = 0.8$  and  $-0.05$  for typical  $M = 0.5$ ) and is not included in the remainder of the analysis.

Figure 1 shows the time evolution of plasma parameters for one of the longest duration discharges achieved thus far in NSTX. Figure 1a shows  $\beta_N$  approaching 6 near  $t=0.9$ s and exceeding 5 for  $t=0.5-1.05$ s. During this time interval, rotational stabilization of the resistive wall mode [8] allows stable operation above the  $n=1$  no-wall stability limit  $\beta_N \approx 3.8-4.2$  computed using the DCON code [21], and several  $n=1$  MHD bursts and rapid but temporary decreases in  $\beta_N$  are observed when  $\beta_N$  exceeds the computed  $n=1$  ideal-wall limit  $\beta_N \approx 5.3-5.7$  late in the high  $\beta_N$  phase. For reference, the peak toroidal beta  $\beta_T$  reaches 17%, the estimated current redistribution time during the high- $\beta_N$  phase is 0.25-0.3s [22], and the energy confinement time  $\tau_E=35$ ms. The neutral beam heating power is held fixed at 6MW from  $t=0.16$ s through the remainder of the discharge, and Figure 1b shows that reduced  $\beta_N$  correlates with enhanced low-frequency  $n=1$  MHD activity. Figure 1c shows that during the high  $\beta_N$  phase the minimum safety factor value decreases very slowly and becomes nearly constant with  $q_0 = q_{min}=1.2-1.3$ . This discharge is in a nearly stationary state with the exception of the plasma density which slowly increases to the Greenwald value [23] as shown in Figure 1a. Simultaneous proximity to the density limit and the ideal-wall stability limit likely plays a role in triggering the MHD activity that ultimately ends the quiescent phase

of the discharge. During the quiescent phase, Figure 1d shows that the total predicted current agrees with the measured total to within 5%. Figure 1d also shows that up to 60% of the current is driven non-inductively by the neoclassical bootstrap effect, neutral beam injection current drive, and toroidal components of the Pfirsch-Schluter and diamagnetic currents. Similar 700kA discharges have achieved 65-70% non-inductive current fraction but do not have complete MSE data sets.

The neoclassical conductivity  $\sigma_{nc}$  and bootstrap current are calculated from theory valid for general geometry and low aspect ratio [24], and the beam current drive is calculated using the TRANSP code [25]. The ohmic current density is calculated from  $\langle \vec{J}_{OH} \cdot \vec{B} \rangle \equiv \sigma_{nc} \langle \vec{E} \cdot \vec{B} \rangle$  where the inductive electric field  $\vec{E} = -\partial\vec{A}/\partial t$  and  $\vec{A}$  is the total (poloidal and toroidal) vector potential obtained from the equilibrium reconstructions [15]. As seen in Figure 2a the profile of the calculated total flux-surface-averaged parallel current density is also in good agreement with the reconstructed profile during the MHD-quiescent phase at high  $\beta_N$ . In contrast, after  $t=1.05s$ , a 5-10kHz continuous  $n=1$  mode becomes unstable and causes a significant decrease in plasma confinement and reduces  $\beta_N$  from 5.5 to 4 as evident in Figures 1a and b. During this same period the density slowly decreases and the electron pressure profile peaking increases. These changes cause the calculated bootstrap and beam-driven currents to increase in the plasma core, and as shown in Figure 2b, the calculated central current density exceeds the reconstructed value by 45%. Since resistive diffusion will tend to continually increase the ohmic current density in the plasma core and drive the minimum  $q$  towards unity, understanding how the experimentally broadened current profile is maintained after  $t=1.05s$  is a key result of this letter.

During the discharge phase when no low-frequency  $n=1$  mode activity is present, the total neutron rate calculated by TRANSP is approximately 10% higher than the measured value but is within the experimental uncertainty of the measurement. The detailed time-evolution of the neutron rate is otherwise in good agreement during this period, and this trend can be used to determine the impact of the MHD activity after  $t=1.05s$ . In Figure 2c the predicted value is renormalized to match the measured value during the time interval  $t=0.8-0.9s$ . From this renormalization it is evident that the onset of late  $n=1$  MHD activity correlates with an additional 20-30% decrease in neutron rate relative to prediction assuming no anomalous fast-ion diffusion is present. From this decrease it is inferred that the late  $n=1$  mode is modifying the fast-ion population and possibly the NBICD.

To gain a better understanding of the structure of the n=1 mode, Ultra-Soft X-Ray (USXR) line-integrated emission data [26] has been inverted [19] to calculate both the equilibrium and perturbed emission profiles. Figure 3a shows the line-integrated emission data in the plasma core during late n=1 mode activity, and Figure 3b shows the best fit to the total emission obtained with a m/n=1/1 kink eigenfunction. Figure 3c shows the time evolution of the best-fit kink flux-surface-normal displacement profile at the outboard midplane. As seen in the figure, the maximum displacement is approximately 1.6cm at  $\rho = 0.4$ . In the modeling, the displacement is constrained to be zero at the plasma edge because the energy-filtered emission is too weak near the plasma boundary to accurately determine the displacement. Despite this limitation, the eigenfunction is evidently initially quite broad with finite amplitude extending to  $\rho \approx 0.8$ , while at later times the eigenfunction narrows to have almost zero displacement outside  $\rho = 0.5$  during mode saturation. After t=1.14s, the eigenfunction shape from USXR inversion is measured to change little, and the poloidal magnetic field fluctuation amplitude measured at the outboard vacuum vessel wall remains approximately constant at 3-5 Gauss RMS.

The core USXR emission cannot be well-fit using a 2/1 island eigenfunction, and it is noteworthy that the 1/1 component is present in a plasma with no  $q = 1$  surface. The reconstructed  $q$  profile is flat to weakly reversed with  $q_0 - q_{min} \approx 0.1$  and  $\rho_{q_{min}} = 0.3 - 0.45$  with the  $q = 2$  surface located near  $\rho = 0.65$ . As shown in Figure 3c, such profiles are calculated to be resistive interchange unstable ( $D_R > 0$ ) at t=1.16s for  $\rho=0.2-0.5$ . Additional analysis finds resistive interchange instability requires  $\beta_N > 3.6$  and  $q_{min} < 1.3$ , and internal n=1 ideal modes become unstable for  $q_{min} < 1.1$  and  $\beta_N > 3.9$ . Thus, the observed mode may be a saturated non-resonant version of the resistive interchange mode [27] or a quasi-interchange mode [28].

The mode magnetic field perturbation amplitude can be estimated from the USXR data [19], and the flux-surface normal component of the perturbed field can be as large as 3% of the modulus of the equilibrium field in the plasma core. Tearing modes [29, 30] and Alfvén instabilities [31] have previously been identified as capable of causing energetic particle diffusion and loss via orbit stochastization, and the interchange-type instability described here apparently provides another mechanism for enhanced fast ion diffusion in the plasma core. Fast ion diffusion can be modeled in TRANSP using a time and spatially dependent diffusivity for the slowing-down ions from NBI. For the time period from t=1.05-

1.15s, Figure 3c shows the eigenfunction radial extent is changing rapidly, and a constant anomalous fast-ion diffusivity  $\chi_{fast} = 15m^2s^{-1}$  extending from  $\rho = 0.0 - 0.7$  can reproduce the measured neutron rate during this time interval. Higher diffusivity values extending over a narrower minor radial extent can also produce similar decrements in predicted neutron rate. After  $t=1.15s$ , the eigenfunction extent remains approximately fixed, and the best simultaneous match to the subsequent neutron rate evolution and reconstructed current density profile is obtained with  $\chi_{fast} = 50m^2s^{-1}$  inside  $\rho = 0.3$ . As seen in Figure 4a, this non-zero fast-ion diffusivity assumption reproduces the measured neutron rate evolution for  $t > 1.05s$ . Perhaps more consistent with the mode extent from the USXR data,  $\chi_{fast} = 20m^2s^{-1}$  inside  $\rho = 0.45$  also reproduces the measured neutron rate. Further, as shown in Figure 4b, this simulated redistribution of fast ions reduces the calculated total current density in the core from 45% higher than the reconstructed value to the same value to within the uncertainty of the calculation. Further, the NBICD density is increased by 20-40% for  $\rho = 0.5-0.6$  resulting in a flat to hollow NBICD profile. The total NBICD and fast-ion stored energy are reduced by only 15% for the two diffusion models shown, so most of the NBICD is apparently redistributed rather than lost.

In summary, the results above demonstrate that core-MHD-induced fast-ion redistribution can convert a centrally peaked NBICD profile into a flat or even hollow profile. This conversion apparently raises the safety factor in the plasma core producing a flat to weakly reversed-shear  $q$  profile which supports core  $n=1$  MHD activity which saturates and helps sustain a broadened NBICD profile and elevated safety factor. It is noteworthy that for the  $q$  profile characteristics described above, interchange modes are potentially self-regulating since they become more unstable as  $q_{min}$  is lowered thereby increasing fast-ion diffusion and raising  $q_{min}$ . Similar mode dynamics and MHD-induced NBICD diffusion may also be relevant to tokamak scenarios proposed for ITER in which 3/2 NTMs have previously been reported to aid sustainment of  $q_0$  above unity for extended durations [32].

This research was supported by the United States Department of Energy under contract numbers DE-AC02-76CH03037 (PPPL), and grant number DE-FG02-99ER54523 (JHU).

---

[1] Y.-K. M. Peng and D. J. Strickler, Nucl. Fus. **26**, 769 (1986).

[2] R. Maingi *et al.*, Phys. Rev. Lett. **88**, 035003 (2002).



- [3] M. Gryaznevich *et al.*, Phys. Rev. Lett. **80**, 3972 (1998).
- [4] S. A. Sabbagh *et al.*, Phys. Plasmas **9**, 2085 (2002).
- [5] J. E. Menard *et al.*, Nucl. Fus. **43**, 330 (2003).
- [6] D. Gates and the NSTX National Research Team, Phys. Plasmas **10**, 1659 (2003).
- [7] J. E. Menard *et al.*, Phys. Plasmas **11**, 639 (2004).
- [8] A. C. Sontag *et al.*, Phys. Plasmas **12**, 056112 (2005).
- [9] D. Gates *et al.*, Nucl. Fus. **46**, S22 (2006).
- [10] M. Murakami *et al.*, Phys. Rev. Lett. **90**, 255001 (2003).
- [11] R. J. Bickerton, J. W. Connor, and J. B. Taylor, Nature Phys. Sci. **229**, 110 (1971).
- [12] M. R. Wade *et al.*, Phys. Plasmas **8**, 2208 (2001).
- [13] A. C. C. Sips *et al.*, Plasma Phys. and Contr. Fus. **44**, B69 (2002).
- [14] E. Joffrin *et al.*, Nucl. Fus. **45**, 626 (2005).
- [15] C. B. Forest *et al.*, Phys. Rev. Lett. **73**, 2444 (1994).
- [16] F. Levinton and H. Yuh, Rev. Sci. Instrum. (2006), in preparation.
- [17] B. W. Rice, K. H. Burrell, and L. L. Lao, Nucl. Fus. **37**, 517 (1997).
- [18] J. E. Menard, Phys. Plasmas (2006), in preparation.
- [19] J. E. Menard *et al.*, Nucl. Fus. **45**, 539 (2005).
- [20] F. L. Hinton and S. K. Wong, Phys. Fluids B **28**, 3082 (1985).
- [21] A. Glasser and M. Chance, Bull. Am. Phys. Soc. **42**, 1848 (1997).
- [22] D. R. Mikkelsen, Phys. Fluids B **1**, 333 (1989).
- [23] M. Greenwald *et al.*, Nucl. Fus. **28**, 2199 (1988).
- [24] O. Sauter, C. Angioni, and Y. R. Lin-Liu, Phys. Plasmas **6**, 2834 (1999).
- [25] R. J. Goldston, D. C. McCune, and H. H. Towner, J. Comput. Phys. **43**, 61 (1981).
- [26] D. Stutman *et al.*, Rev. Sci. Instrum. **70**, 572 (1999).
- [27] M. S. Chu *et al.*, Phys. Rev. Lett. **77**, 2710 (1996).
- [28] C. Wahlberg, Plasma Phys. and Contr. Fus. **47**, 757 (2005).
- [29] C. B. Forest *et al.*, Phys. Rev. Lett. **79**, 427 (1997).
- [30] E. M. Carolipio, W. W. Heidbrink, C. B. Forest, and R. B. White, Nucl. Fus. **42**, 853 (2002).
- [31] K. L. Wong *et al.*, Phys. Rev. Lett. **93**, 085002 (2004).
- [32] T. C. Luce and DIII-D Team, Nucl. Fus. **45**, S86 (2005).

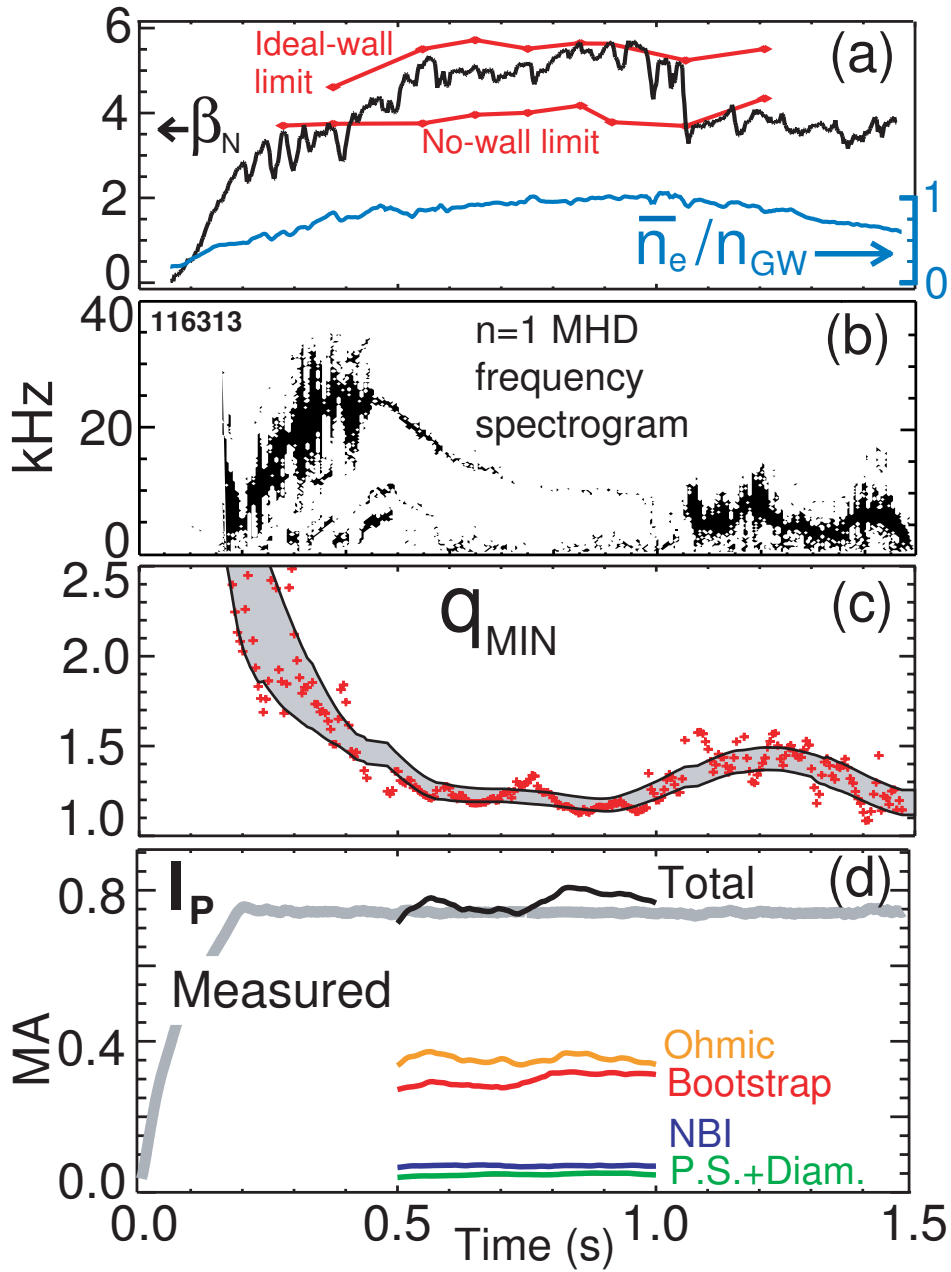


FIG. 1: (a) Normalized beta (black), calculated  $n=1$  no-wall and ideal-wall stability limits (red), and line-average density normalized to Greenwald value (blue), (b)  $n=1$  MHD activity frequency spectrogram, (c) reconstructed instantaneous (red) and 200ms time-average (gray) minimum  $q$  value, (d) measured (gray) and calculated total (black) plasma currents with inductive and non-inductive contributions also plotted.

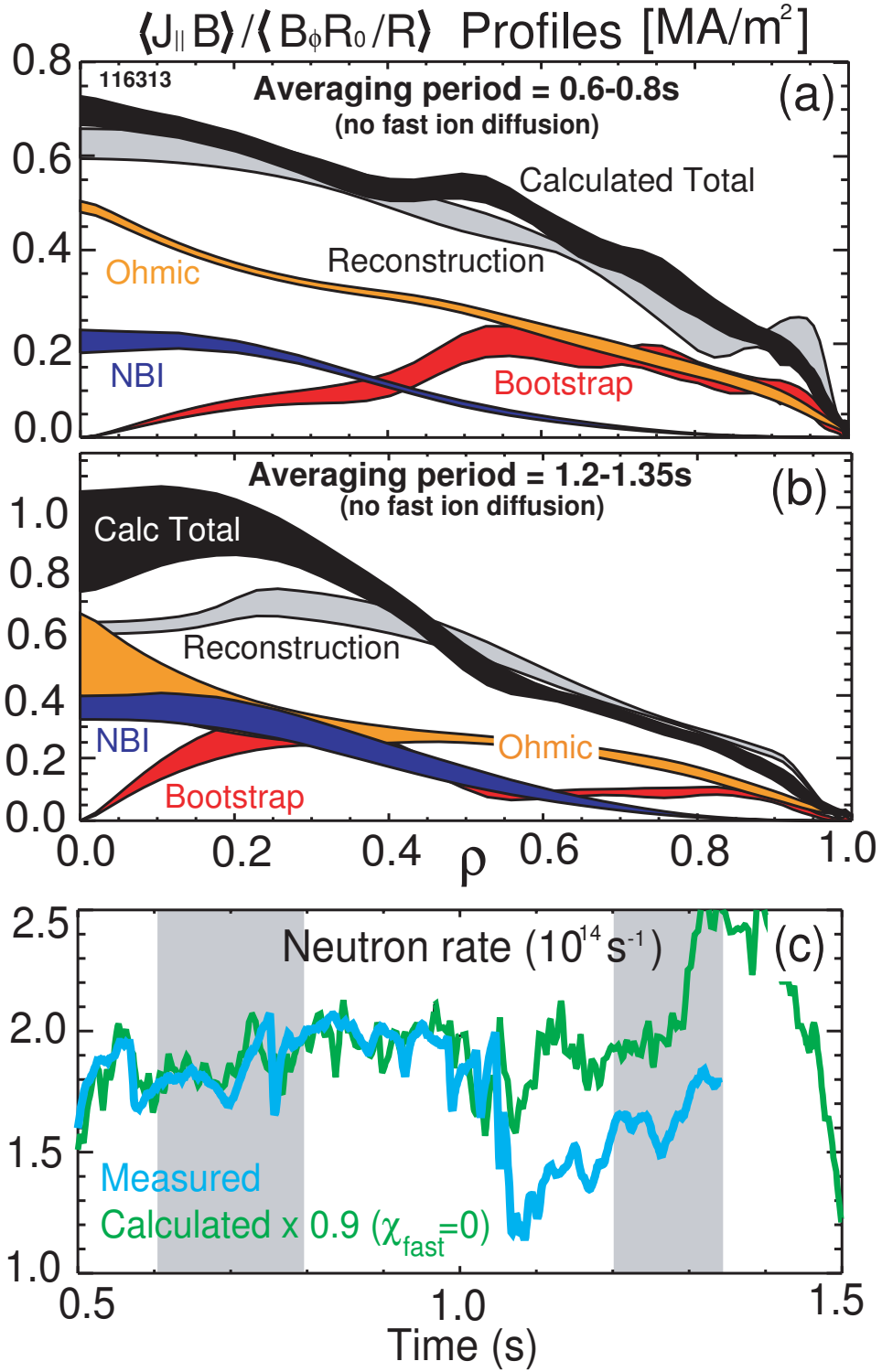


FIG. 2: (a) Comparison of the time-averaged reconstructed (gray) and calculated (black) parallel current density profile from  $t=0.6-0.8\text{s}$ , (b) from  $t=1.2-1.35\text{s}$ , and (c) measured (blue) and calculated (green) neutron rates assuming no anomalous fast ion diffusion.

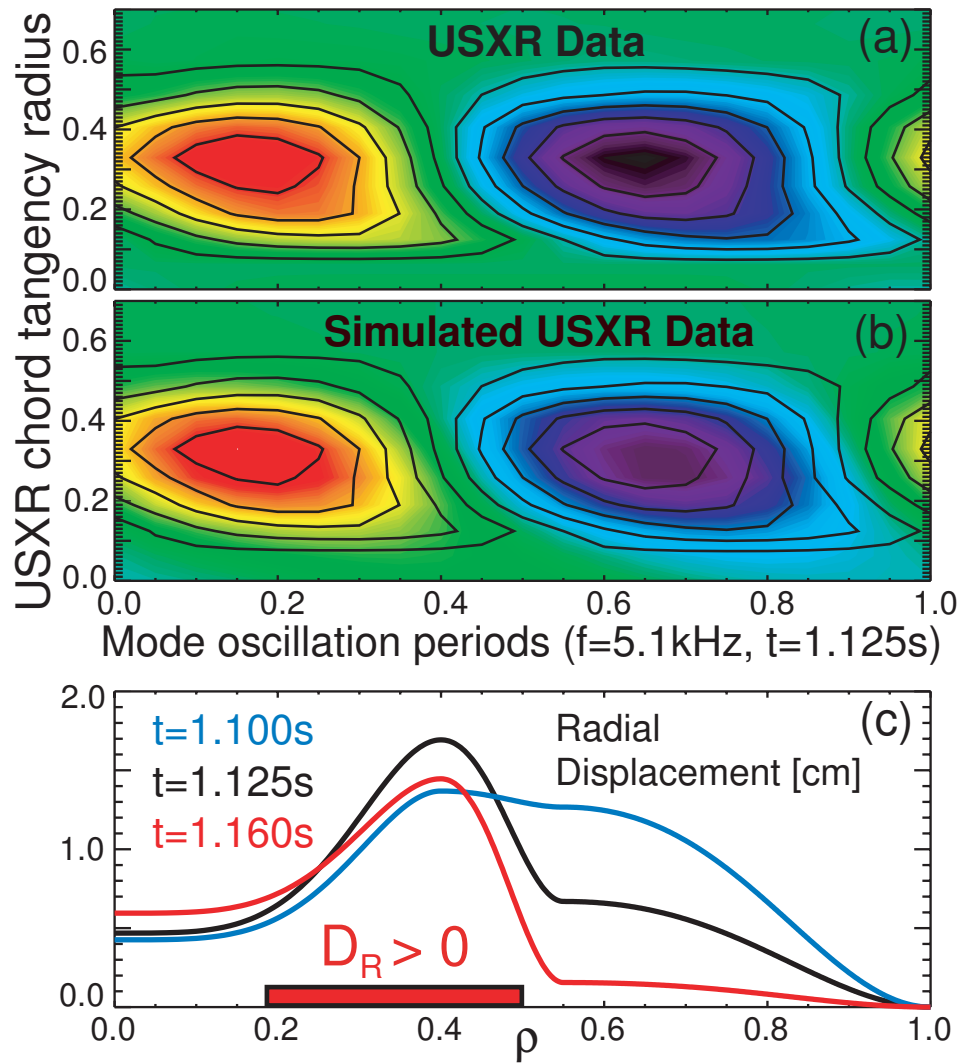


FIG. 3: (a) Measured line-integrated USXR emission amplitude contours plotted versus chord tangency  $\rho$  and time for one oscillation period, (b) best-fit simulated USXR emission amplitude assuming a 1/1 kink eigenfunction, and (c) reconstructed kink radial displacement amplitude profile at outboard midplane during mode saturation.

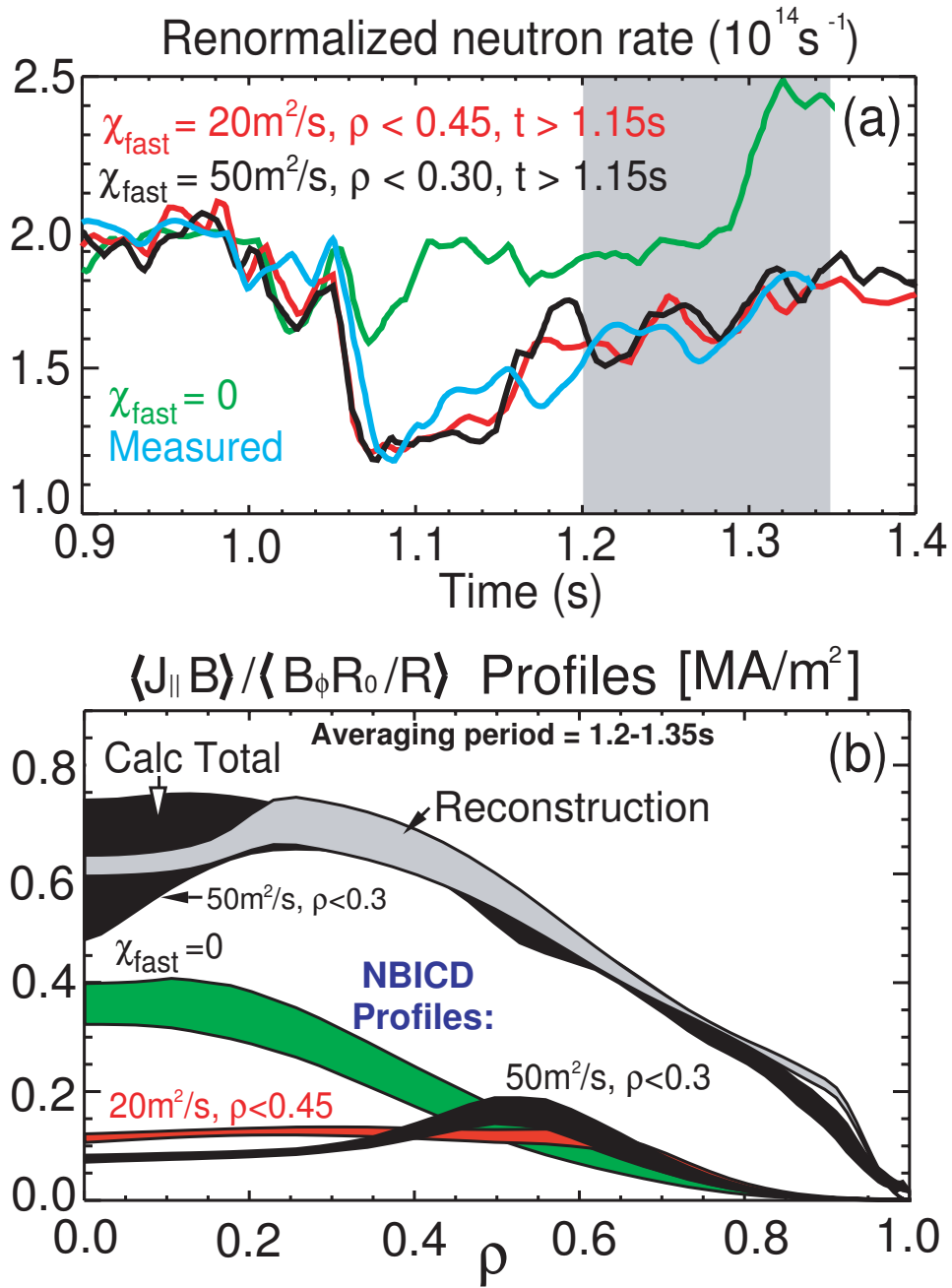


FIG. 4: (a) Comparison of the measured (blue) to calculated neutron rate, and (b) comparison of reconstructed (gray) and calculated total (black) parallel current density profile for  $t=1.2-1.35\text{s}$  for the best-fit fast-ion diffusivity model. NBICD profiles for the diffusivities of (a) are also shown.



## External Distribution

Plasma Research Laboratory, Australian National University, Australia  
Professor I.R. Jones, Flinders University, Australia  
Professor João Canalle, Instituto de Fisica DEQ/IF - UERJ, Brazil  
Mr. Gerson O. Ludwig, Instituto Nacional de Pesquisas, Brazil  
Dr. P.H. Sakanaka, Instituto Fisica, Brazil  
The Librarian, Culham Science Center, England  
Mrs. S.A. Hutchinson, JET Library, England  
Professor M.N. Bussac, Ecole Polytechnique, France  
Librarian, Max-Planck-Institut für Plasmaphysik, Germany  
Jolan Moldvai, Reports Library, Hungarian Academy of Sciences, Central Research  
Institute for Physics, Hungary  
Dr. P. Kaw, Institute for Plasma Research, India  
Ms. P.J. Pathak, Librarian, Institute for Plasma Research, India  
Dr. Pandji Triadyaksa, Fakultas MIPA Universitas Diponegoro, Indonesia  
Professor Sami Cuperman, Plasma Physics Group, Tel Aviv University, Israel  
Ms. Clelia De Palo, Associazione EURATOM-ENEA, Italy  
Dr. G. Grosso, Istituto di Fisica del Plasma, Italy  
Librarian, Naka Fusion Research Establishment, JAERI, Japan  
Library, Laboratory for Complex Energy Processes, Institute for Advanced Study,  
Kyoto University, Japan  
Research Information Center, National Institute for Fusion Science, Japan  
Professor Toshitaka Idehara, Director, Research Center for Development of Far-Infrared Region,  
Fukui University, Japan  
Dr. O. Mitarai, Kyushu Tokai University, Japan  
Mr. Adefila Olumide, Ilorin, Kwara State, Nigeria  
Dr. Jiangang Li, Institute of Plasma Physics, Chinese Academy of Sciences, People's Republic of China  
Professor Yuping Huo, School of Physical Science and Technology, People's Republic of China  
Library, Academia Sinica, Institute of Plasma Physics, People's Republic of China  
Librarian, Institute of Physics, Chinese Academy of Sciences, People's Republic of China  
Dr. S. Mirnov, TRINITI, Troitsk, Russian Federation, Russia  
Dr. V.S. Strelkov, Kurchatov Institute, Russian Federation, Russia  
Kazi Firoz, UPJS, Kosice, Slovakia  
Professor Peter Lukac, Katedra Fyziky Plazmy MFF UK, Mlynska dolina F-2, Komenskeho Univerzita,  
SK-842 15 Bratislava, Slovakia  
Dr. G.S. Lee, Korea Basic Science Institute, South Korea  
Dr. Rasulkhozha S. Sharafiddinov, Theoretical Physics Division, Institute of Nuclear Physics, Uzbekistan  
Institute for Plasma Research, University of Maryland, USA  
Librarian, Fusion Energy Division, Oak Ridge National Laboratory, USA  
Librarian, Institute of Fusion Studies, University of Texas, USA  
Librarian, Magnetic Fusion Program, Lawrence Livermore National Laboratory, USA  
Library, General Atomics, USA  
Plasma Physics Group, Fusion Energy Research Program, University of California at San Diego, USA  
Plasma Physics Library, Columbia University, USA  
Alkesh Punjabi, Center for Fusion Research and Training, Hampton University, USA  
Dr. W.M. Stacey, Fusion Research Center, Georgia Institute of Technology, USA  
Director, Research Division, OFES, Washington, D.C. 20585-1290

The Princeton Plasma Physics Laboratory is operated  
by Princeton University under contract  
with the U.S. Department of Energy.

Information Services  
Princeton Plasma Physics Laboratory  
P.O. Box 451  
Princeton, NJ 08543

Phone: 609-243-2750  
Fax: 609-243-2751  
e-mail: [pppl\\_info@pppl.gov](mailto:pppl_info@pppl.gov)  
Internet Address: <http://www.pppl.gov>